Mycobacterial catalase–peroxidase is a tissue antigen and target of the adaptive immune response in systemic sarcoidosis

Zhimin Song,[1] Lisa Marzilli,[2] Brian M. Greenlee,[1] Edward S. Chen,[1] Richard F. Silver,[5] Frederic B. Askin,[3] Alvin S. Teirstein,[6] Ying Zhang,[4] Robert J. Cotter,[2] and David R. Moller[1]

[1]Division of Pulmonary and Critical Care Medicine, Department of Medicine, [2]Department of Pharmacology and Molecular Sciences, [3]Department of Pathology, and [4]Department of Molecular Microbiology and Immunology, The Johns Hopkins University Bloomberg School of Public Health, The Johns Hopkins University School of Medicine, Baltimore, MD 21205
[5]Department of Medicine, Case Western Reserve School of Medicine, Cleveland, OH 441063
[6]Division of Pulmonary and Critical Care Medicine, Mount Sinai Medical Center, New York, NY 10029

Sarcoidosis is a disease of unknown etiology characterized by noncaseating epithelioid granulomas, oligoclonal CD4$^+$ T cell infiltrates, and immune complex formation. To identify pathogenic antigens relevant to immune-mediated granulomatous inflammation in sarcoidosis, we used a limited proteomics approach to detect tissue antigens that were poorly soluble in neutral detergent and resistant to protease digestion, consistent with the known biochemical properties of granuloma-inducing sarcoidosis tissue extracts. Tissue antigens with these characteristics were detected with immunoglobulin (Ig)G or F(ab′)$_2$ fragments from the sera of sarcoidosis patients in 9 of 12 (75%) sarcoidosis tissues (150–160, 80, or 60–64 kD) but only 3 of 22 (14%) control tissues (all 62–64 kD; P = 0.0006). Matrix-assisted laser desorption/ionization time of flight mass spectrometry identified *Mycobacterium tuberculosis* catalase–peroxidase (mKatG) as one of these tissue antigens. Protein immunoblotting using anti-mKatG monoclonal antibodies independently confirmed the presence of mKatG in 5 of 9 (55%) sarcoidosis tissues but in none of 14 control tissues (P = 0.0037). IgG antibodies to recombinant mKatG were detected in the sera of 12 of 25 (48%) sarcoidosis patients compared with 0 of 11 (0%) purified protein derivative (PPD)$^-$ (P = 0.0059) and 4 of 10 (40%) PPD$^+$ (P = 0.7233) control subjects, suggesting that remnant mycobacterial catalase–peroxidase is one target of the adaptive immune response driving granulomatous inflammation in sarcoidosis.

CORRESPONDENCE
David R. Moller:
dmoller@jhmi.edu

Abbreviations used: BCG, Bacille Calmette-Guerin; DIG, digoxigenin; HRP, horseradish peroxidase; ISH, in situ hybridization; MALDI-TOF, matrix-assisted laser desorption/ionization time of flight; mHsp65, *Mycobacterium bovis* Hsp65 protein; mKatG, *Mycobacterium tuberculosis* catalase–peroxidase; MOWSE, mol wt search; *Mtb*, *Mycobacterium tuberculosis*; Pe, precipitated cell pellets; PK, proteinase K; PPD, purified protein derivative; TSA, tyramide signal amplification; TX100, Triton X-100.

Sarcoidosis is recognized as an immune-mediated granulomatous disease because tissue inflammation involves activated CD4$^+$ T cells and mononuclear cells with giant cell formation (1). This inflammatory response is associated with marked skewing of the cytokine response toward a Th1 cell cytokine profile with enhanced expression of IFN-γ, IL-2, and TNF along with the Th1 cell regulatory cytokines, IL-12 and IL-18 (2–4). Studies of TCR gene expression in sarcoidosis provide evidence that oligoclonal populations of αβ$^+$ CD4$^+$ T cells collect at sites of granulomatous inflammation, consistent with an MHC-restricted antigen-driven response (5–7). Concomitant stimulation of the adaptive B cell response in sarcoidosis is evidenced by the immune complex formation found in 70–100% of patients early in this disorder (8). Although the identity of the stimulating antigens in sarcoidosis remains unknown, experimental models indicate that adaptive Th1/Th2 cell responses mediate immune-mediated granulomatous inflammation (9, 10).

A major step in understanding the etiopathogenesis of sarcoidosis would be the identification of specific antigens contributing to the adaptive immune response mediating granulomatous inflammation in this disease. To identify potential target antigens of the adaptive immune response in sarcoidosis, we have capitalized on the observation that homogenates of diseased tissue injected intradermally in patients with sarcoidosis elicit a nidus of granulomatous inflammation that is indistinguishable from spontane-

L. Marzilli's present address is Wyeth Biopharma Co., Andover, MA 01810.

The online version of this article contains supplemental material.

ously arising granulomas, known as the Kveim (or Kveim-Siltzbach) reaction (11–13). In this reaction, well-formed epithelioid granulomas develop after 2–4 wk. In timing and histopathology, this granulomatous response is analogous to the Mitsuda reaction to lepromins in tuberculoid leprosy (14). Early studies found circulating antibodies were directed against the Kveim reagent, consistent with a humoral response to antigens present in sarcoidosis tissue (15). Our own studies demonstrated the presence of expanded populations of clonal T cells at Kveim reaction sites, consistent with antigen-specific responses to components in Kveim extracts (16). Biochemical characteristics of granuloma-inducing Kveim extracts include neutral detergent insolubility, relative heat, acid, and protease resistance, and sensitivity to potent denaturants, consistent with poorly soluble protein aggregates (17, 18). In this study, we used a limited proteomic approach with protein immunoblot and matrix-assisted laser desorption/ionization time of flight (MALDI-TOF) mass spectrometry to identify potential antigenic targets in sarcoidosis tissue that may contribute to immune-mediated granulomatous inflammation in sarcoidosis.

RESULTS

Protease-resistant proteins in sarcoidosis tissues are targets of circulating IgG

To enrich for tissue antigens associated with sarcoidosis granuloma formation, we used the known biochemical properties of active Kveim reagent to limit the target proteome by preparing Triton X-100 (TX100) detergent-insoluble extracts of sarcoidosis and control lymph node homogenates with or without proteinase K (PK) digestion (17, 18). When non-PK–treated tissue extracts were solubilized and analyzed by protein immunoblot, multiple antigenic bands were seen using sarcoidosis or control total IgG or $F(ab')_2$ fragments detected with anti-Fc or anti-Fab reagents (Fig. 1). When the same sarcoidosis tissue homogenates were digested with PK overnight, we found discrete bands in six of nine (67%) lymph node, one lung, and two spleen samples that were not detected with secondary antibody alone (Table I and Fig. 1, A–D). The antigenic bands varied in size with 60-, 62–64-, 80-, or ~150–160-kD bands seen in different samples (Table I). In one of these samples, the 62–64-kD bands (but not other bands) were detected with control sera. Analysis of nonsarcoidosis control tissues demonstrated that only 1 of 11 (9%) lymph node, 1 of 5 (20%) splenic, and 0 of 1 lung samples with PK-resistant antigenic bands were detected using sarcoidosis sera as detecting reagent. In both of these cases, 62–64-kD bands were seen, suggesting that these antigens were not exclusive to sarcoidosis tissues. Overall, 9 of 12 (75%) sarcoidosis tissue samples but only 2 of 17 (12%) control tissue samples contained TX100-insoluble, PK-resistant antigenic bands detected with sarcoidosis IgG or $F(ab')_2$ fragments ($P = 0.0013$).

Sarcoidosis tissue antigens are poorly soluble in a moderately denaturing detergent

In addition to the TX100 detergent extraction method to isolate potential disease-relevant antigens in sarcoidosis tissues, as a second approach we used a sarkosyl-based extraction procedure designed to enrich for poorly soluble protein (prion) aggregates (19). Two sarcoidosis and seven control samples with sufficient amounts of tissue to complete this protocol were analyzed. We found multiple antigenic bands in the initial insoluble fraction (P22) and intermediate supernatant fraction (S215) from both sarcoidosis and control tissues using sarcoidosis IgG reagents (Fig. 2). When the final precipitated cell pellets (Pe) were solubilized and subjected to protein immunoblotting, we found antigenic bands in both of the sarcoidosis tissues (Fig. 2 and Table I). The sarcoidosis spleen sample demonstrated four antigenic bands similar in size to those detected using the TX100/PK digestion protocol (Fig. 2 A and Table I). The sarcoidosis lung sample yielded antigenic bands (60, 62, and ~160 kD) in the final Pe fraction (Fig. 2 B and Table I). The Pe fractions

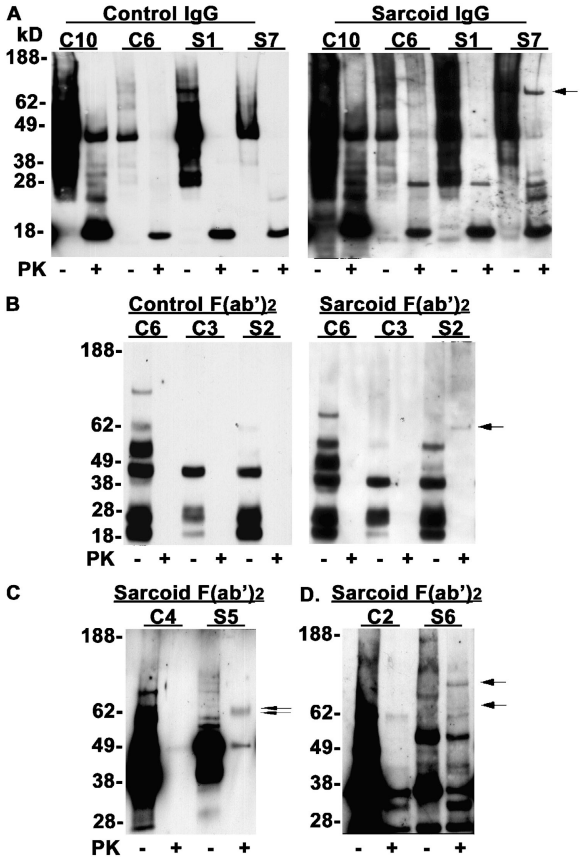

Figure 1. Protease-resistant proteins in sarcoidosis tissues are targets of circulating IgG from patients with sarcoidosis. TX100-insoluble detergent extracts from sarcoidosis (S) and control (C) lymph nodes were treated with or without PK and subjected to denaturing SDS-PAGE and immunoblot analysis with purified IgG or $F(ab')_2$ fragments from pooled control or sarcoidosis sera detected with anti–human Fcγ or Fab reagents, respectively. Four separate immunoblots (A–D) with samples corresponding to Table I are shown. Immunoblots in A and B were probed with control reagents, stripped, and then reprobed with sarcoidosis reagents. Numbers give molecular mass in kilodaltons (kD). Arrows demark antigenic bands in PK-treated sarcoidosis tissues when probed with sarcoidosis serologic reagents but not control reagents or secondary antibody alone.

Table I. Summary of antigenic bands from protein immunoblots of extracts of sarcoidosis and control tissues

Sample		Pathology	Extraction	Detecting sera		Antigenic bands (kD)	Anti-mKatG (IT57)
				Sarcoidosis	Control		
Sarcoidosis							
S1	LN[a]	NCG[b]	TX100	−[c]	−	none	−
S2	LN	NCG	TX100	+	−	60	+
S3	LN	NCG	TX100	+	ND	62, 64	−
S4	LN	NCG	TX100	−	ND	none	ND
S5	LN	NCG	TX100	+	−	62, 64	+
S6	LN	NCG	TX100	+	ND	62, 64, 80	−
S7	LN	NCG	TX100	+	ND	∼160	ND
S8	LN	NCG	TX100	+	−	62	ND
S9	LN	no gran[d]	TX100	−	−	none	−
S10	SPL[e]	NCG	TX100	+	−	60, 62	+
S11	SPL	NCG	TX100	+	+	60, 62[f], 64[f], 150, 160	
			Sarkosyl	+	+	60, 62[f], 64[f], 150, 160	+
S12	LU[g]	NCG	TX100	+	ND	∼160	
			Sarkosyl	+	−	60, 62, ∼160	+
Controls							
C1	LN	no path[h]	TX100	−	−	none	ND
C2	LN	no path	TX100	+	−	62	−
C3	LN	no path	TX100	−	−	none	−
C4	LN	no path	TX100	−	−	none	−
C5	LN	no path	TX100	−	−	none	−
C6	LN	FH[i]	TX100	−	−	none	−
C7	LN	FH	TX100	−	ND	none	ND
C8	LN	no path	TX100	−	ND	none	−
C9	LN	no path	TX100	−	ND	none	−
C10	LN	no path	TX100	−	−	none	−
C11	LN	no path	TX100	−	ND	none	ND
C12	SPL	no path	TX100	−	ND	none	−
C13	SPL	no path	TX100	−	−	none	−
C14	SPL	no path	Sarkosyl	−	ND	none	ND
C15	SPL	no path	Sarkosyl	−	−	none	ND
C16	SPL	no path	Sarkosyl	−	−	none	ND
C17	SPL	no path	Sarkosyl	−	ND	none	−
C18	SPL	no path	TX100	−	−	none	−
C19	SPL	no path	TX100	−	ND	none	
			Sarkosyl	+	+	62[f], 64[f]	−
C20	SPL	no path	Sarkosyl	−	−	none	ND
C21	SPL	no path	TX100	+	ND	62, 64	ND
C22	LU	no path	TX100	−	ND	none	−
			Sarkosyl	−	ND	none	−

[a]Lymph node.
[b]Noncaseating granuloma.
[c]−, no clearly detectable band; +, presence of bands not seen with secondary antibody alone.
[d]No granuloma.
[e]Spleen.
[f]Bands also seen with control sera.
[g]Lung.
[h]No tumor, granuloma, or other identified pathology.
[i]Follicular hyperplasia.

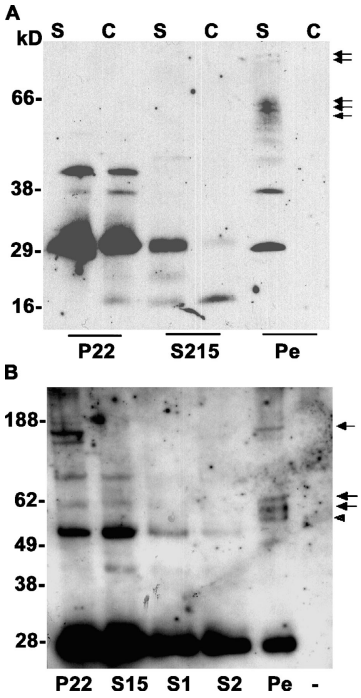

Figure 2. Sarcoidosis tissues extracted with sarkosyl contain poorly soluble protein antigens that bind to sarcoidosis IgG. (A) Protein fractions from sarcoidosis (S) or control (C) spleen. (B) Protein fractions from sarcoidosis lung. Protein fractions were analyzed by protein immunoblotting using purified IgG from sarcoidosis sera detected with anti-human Fcγ reagents. The initial homogenates (P22), intermediate supernatant fractions (S215, S1, and S2), or final cell pellets that were poorly soluble in sarkosyl (Pe) are shown. Pe were solubilized using 8 M urea plus β-mecaptoethanol and were precipitated before analysis by gel electrophoresis. Arrows point to antigenic bands seen in the Pe fractions of sarcoidosis but not control tissues. Arrowhead points to a 56-kD band detected with anti-Fcγ reagents alone in the Pe fraction from sarcoidosis lung (B).

from five of six control spleens (Fig. 2 A) and one control lung (not depicted) that were processed in parallel contained little detectable protein and did not demonstrate antigenic bands using either sarcoidosis or control IgG reagents (Table I). One control spleen sample demonstrated 62–64-kD bands reactive with both sarcoidosis and control sera. Overall, combining results from both the sarkosyl and TX100 extraction procedures, we found that 9 of 12 (75%) sarcoidosis tissue samples versus 3 of 22 (14%) control tissue samples demonstrated antigenic bands detected by sarcoidosis sera on immunoblot analysis ($P = 0.0006$).

Identification of candidate pathogenic antigens using MALDI-TOF mass spectrometry

To identify these candidate pathogenic tissue antigens, two sarcoidosis tissues with sufficient amounts of remaining processed material were analyzed. Gel slices of the approximate size of the antigenic bands were excised, subjected to in situ trypsin digestion, and analyzed by MALDI-TOF mass spectrometry. The mass spectrum of the trypsin digest of a 60–62-kD sized gel slice from the Pe fraction from a sarcoidosis spleen extract (Fig. 2 A, S11) demonstrated multiple peaks that were not present in the trypsin control samples, consistent with a complex mixture of peptides. When the peptide mass fingerprints were submitted for protein database sequence analyses, the highest match was for *Mycobacterium tuberculosis* (*Mtb*) catalase–peroxidase (mKatG; mol wt = 80,625; Genpept accession no. U06265). Under low salt precipitation, 8 of 31 (25%) peptide peaks matched this protein (mol wt search [MOWSE] score of $4.89 \times 10e{+}03$). For the combined low and high salt peptide precipitations, 16 of 74 peptides matched the peptide fingerprint of mKatG (MOWSE score of $1.07 \times 10e{+}09$; Mascot score of 71; $P < 0.05$; Table II). Consistent with the presence of myco-

Table II. Summary of peptide matches for mKatG using MALDI-TOF mass spectrometry of sarcoidosis spleen tissue[a]

m/z submitted	MH^+ matched	δ ppm	Start	End	Peptide sequence
562.5000	562.2949	364.7568	485	489	(R)GSDKR(G)
833.2000	833.4634	−315.9844	687	693	(K)VKWTGSR(V)
1163.7000	1163.5420	135.7729	105	114	(R)MAWHAAGTYR(I)
1437.1000	1437.7603	−459.2364	558	571	(K)AAGHNITVPFTPGR(T)
1475.9000	1475.7382	109.6406	706	719	(R)ALVEVYGADDAQPK(F)
1708.3000	1707.9295	216.9512	555	571	(K)AAKAAGHNITVPFTPGR(T)
1713.9000	1713.8124	51.0985	397	410	(R)WLEHPEELADEFAK(A)
1741.6000	1741.8345	−134.6375	105	119	(R)MAWHAAGTYRIHDGR(G)
1774.3000	1774.7938	−278.2053	28	42	(K)YPVEGGGNQDWWPNR(L)
1869.8000	1869.9135	−60.7182	396	410	(R)RWLEHPEELADEFAK(A)
1901.1000	1901.9510	−447.4279	129	145	(R)FAPLNSWPDNASLDKAR(R)
1947.0000	1947.9664	−496.0873	520	537	(R)TLEEIQESFNSAAPGNIK(V)
2018.9000	2018.0963	398.2698	596	613	(R)NYLGKGNPLPAEYILLDK(A)
2342.3000	2343.1517	−363.5002	159	179	(K)LSWADLIVFAGNCALESMGFK(T)
2445.2000	2446.1574	−391.3758	120	143	(R)GGAGGGMQRFAPLNSWPDNASLDK(A)
2470.5000	2471.2467	−302.1548	158	179	(K)KLSWADLIESMGFK(T)

[a]Peptides from the high salt precipitate are shown if both low and high salt precipitates resulted in peptide peaks of similar size (<1 dalton).

bacterial antigens in this sample, when the 16 fragments that matched mKatG were removed and the search was repeated, a top potential match was found to *Mtb* topoisomerase I with 9 matching peptides (Genpept accession no. U40159; MOWSE score of 8.38e+005; Table S1, available at http://www.jem.org/cgi/content/full/jem.20040429/DC1).

Next, we performed MALDI-TOF mass spectrometric analysis of a trypsin digest of a 60–62-kD band excised from the gel of the Pe fraction of a sarcoidosis lung sample from a different patient (Fig. 2 B, S12). Although there was not a single high probability match of the peptide fingerprint from this sample to the database, the MALDI-TOF mass spectrum matched 4 of 26 peptide fragments from *Mycobacterium smegmatis* KatG (MOWSE score of 1.39 × 10e+03; Genpept accession no. 11255575; Table S2). Three other potential antigenic bands (~64, 150, and 160 kD) from this sample provided no statistically significant matches. When gel slices of 60–62 kD in size were excised from five control tissue extracts, the mass spectra demonstrated few peaks, all of very low intensity, that were insufficient for mass spectra fingerprinting analysis.

Confirmation of the presence of mKatG protein in sarcoidosis tissue by protein immunoblot

To independently validate the mKatG results from the peptide fingerprinting analyses and assess the hypothesis that mKatG is a common tissue antigen in sarcoidosis, we analyzed protein immunoblots of sarcoidosis and control tissue extracts using the IT57 mAb reactive to mKatG (20). For reference, recombinant mKatG was denatured by ethanol precipitation and analyzed by protein immunoblot along with heat-sonicated extracts from several mycobacterial and bacterial extracts (Fig. S1, available at http://www.jem.org/cgi/content/full/jem.20040429/DC1). The IT57 mAb reacted strongly to recombinant mKatG, detecting both the ~80-kD monomer and a ~160-kD protein, consistent with homodimer formation known for its native form (21, 22). Additional ~140-, 60-, 56-, and 40-kD peptides derived from mKatG as determined by MALDI-TOF mass spectrometry were also seen (not depicted). The IT57 mAbs reacted strongly to ~80- and ~160-kD proteins from *Mtb* and *M. smegmatis* extracts but did not bind to proteins from *Mycobacterium chelonei*, *Helicobacter pylori*, or *Escherichia coli* (Fig. S1). Protein immunoblots of the same sarcoidosis spleen sample (S11) from which mKatG peptides were detected by MALDI-TOF mass spectrometry demonstrated ~80- and ~160-kD bands, consistent with monomer and homodimer forms of mKatG (Fig. 3). Five control splenic tissues that were processed similarly did not have detectable bands on immunoblot analysis (Fig. 3, C14). Reprobing an immunoblot of the sarcoidosis lung homogenate that yielded a possible match to *M. smegmatis* KatG on MALDI-TOF mass spectrometry demonstrated a faint band of an ~80-kD size. A control lung sample did not bind to IT57 mAb (not depicted). Three of eight (38%) sarcoidosis lymph node but none of the eight (0%) control lymph node samples had detectable bands, consistent with the presence of mKatG protein (Fig. 3, S2 and C2). Other tissue samples could not be reanalyzed because of technically inadequate reprobing of archived immunoblots or lack of biopsy tissue. Overall, 5 of 9 (56%) sarcoidosis tissues compared with 0 of 14 (0%) control tissues had detectable mKatG on protein immunoblotting using anti-mKatG mAbs ($P = 0.0037$).

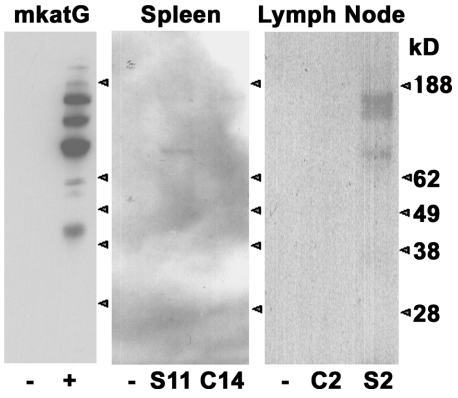

Figure 3. Immunoblot analysis confirms the presence of mKatG protein in sarcoidosis tissue. Shown are individual protein immunoblots of recombinant mKatG, sarkosyl-extracted sarcoidosis (S11), or control (C14) spleen extracts or TX100-insoluble sarcoidosis (S2) or control (C2) lymph node extracts using the IT57 anti-mKatG mAb. Arrowheads demark migration of corresponding mol wt. markers.

In situ hybridization (ISH) demonstrates *Mtb katG* and *16S rRNA* DNA in sarcoidosis tissues

To further substantiate the potential significance of mKatG as a tissue antigen in sarcoidosis, we examined archival biopsy tissues for *mkatG* DNA. Using ISH–tyramide signal amplification (TSA), *mkatG* DNA was detected in 7 of 18 (39%) sarcoidosis and 4 of 4 *Mtb*-infected tissues but not in 0 of 18 control tissues that included 5 biopsies from patients with Wegener granulomatosis (sarcoidosis vs. nontuberculous controls; $P = 0.0076$; Fig. 4 and Table III). Reverse DNA probes and probes from *H. pylori 16S rRNA* were negative in all samples. ISH without signal amplification using probes derived from *Mtb 16S rRNA* confirmed the presence of mycobacterial DNA in 5 of 6 (83%) $mKatG^+$ samples and overall in 6 of 16 (38%) sarcoidosis tissues compared with 0 of 16 (0%) control tissues ($P = 0.018$; Fig. 5 and Table III). Reverse *Mtb 16S rRNA* probes were uniformly negative in all samples.

Sarcoidosis IgG binds recombinant mKatG

To determine the extent to which mKatG is a relevant pathogenic antigen in sarcoidosis, we analyzed sera from sarcoidosis patients and purified protein derivative $(PPD)^+$ and PPD^- control individuals for binding to recombinant mKatG. We found circulating anti-mKatG IgG in the sera of 12 of 25 (48%) sarcoidosis patients compared with 0 of 11 (0%) PPD^- healthy control individuals ($P = 0.0059$) and 4 of 10 (40%) PPD^+ individuals ($P = 0.7233$; overall group com-

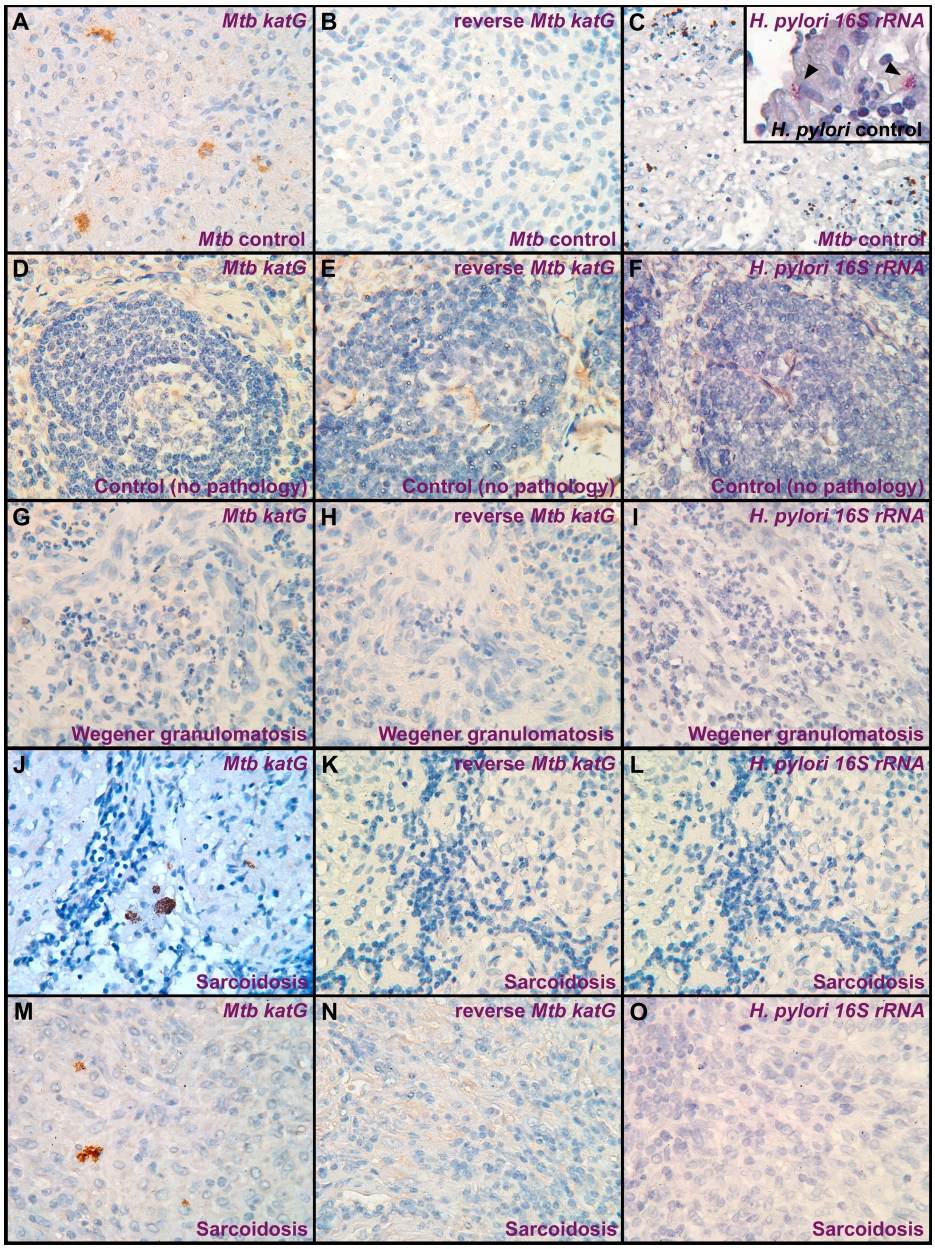

Figure 4. Cellular localization of *mkatG* DNA by ISH with TSA. Shown are representative photomicrographs from biopsies of *Mtb*-infected tissue (A–C), normal controls (no pathology; D–F), Wegener granulomatosis (G–I), and sarcoidosis tissues (J–O). Tissue sections were hybridized with or without DIG-labeled probes, detected with anti-DIG $F(ab')_2$ fragments conjugated with HRP, and the signal was amplified by incubation with biotinylated tyramine followed by streptavidin conjugated to HRP and a DAB chromogen solution. *Mtb*-infected tissue (A) and sarcoidosis samples (J and M) demonstrated focal collections of *mkatG* DNA that were not seen in biopsies from Wegener granulomatosis (G) nor in nongranulomatous control tissues (D). All tissues were negative using reverse *mkatG* and *H. pylori 16S rRNA* probes (C, inset, positive *H. pylori* control).

parison, P = 0.0034; Fig. 6 A and complete data in Table IV). Circulating IgG from both sarcoidosis patients and PPD^+ individuals bound to either 80- or 60-kD mKatG-migrating proteins or both. Two sarcoidosis patients and one PPD^+ individual had positive mKatG immunoblots with serologic titers >1:1,000 (Table IV). Sarcoidosis patients with circulating IgG to mKatG were clinically diverse, including those with and without extrapulmonary involvement. There was no correlation between the presence or absence of anti-mKatG IgG and the radiographic stage of the same patient (Table IV; P = 0.9289).

To determine whether reactivity to mKatG was selective in sarcoidosis or associated with reactivity to other mycobacterial proteins, we analyzed circulating IgG binding to recombinant *Mycobacterium bovis* Hsp65 protein (mHsp65) in these groups. We found circulating IgG binding to mHsp65

Table III. Quantification of focal collections of *mkatG* and *Mtb 16S rRNA* DNA in sarcoidosis and control tissues

					mkatG forward probe		*Mtb 16S rRNA* forward probe		*H. pylori 16S rRNA* forward probe	
Group	Sample	Tissue	Pathology[a]	Fields viewed[b]	Focal collections[c]	Interpretation[d]	Focal collections[c]	Interpretation[d]	Focal collections[c]	Interpretation[d]
Mtb	1	pleura	CAS + NC	32	6	+			0	−
	2	lung	CAS + NC	14	3	+	0	−	0	−
	3	liver	CAS + NC	32	>30	+	10	+	0	−
	4	lung	CAS + NC	32	>30	+	10	+	0	−
Control	1	lung	diff-GC	40	0	−	0	−	0	−
Wegener granulomatosis	2	lung	diff-GC	24	0	−	0	−	0	−
	3	lung	diff-GC	40	0	−	0	−	0	−
	4	lung	diff-GC	32	1	−	0	−	0	−
	5	lung	diff-GC	28	0	−				
Control	1	lung	F	36	0	−	0	−	0	−
UIP	2	lung	Int + F	24	0	−	0	−	0	−
	3	lung	F	24	0	−	0	−	0	−
	4	lung	F	24	0	−			0	−
Control	1	lung	none	24	0	−	0	−	0	−
No pathology	2	lung	none	24	0	−	0	−	0	−
	3	lung	none	20	0	−	0	−	0	−
	4	lung	none	20	0	−	0	−	0	−
	5	LN	none	36	0	−	0	−	0	−
	6	LN	none	24	0	−	0	−	0	−
	7	LN	none	24	0	−	0	−	0	−
	8	LN	none	24	0	−	0	−	0	−
	9	LN	none	20	0	−	0	−	0	−
Sarcoidosis	1	lung	NC	48	12	+	5	+	0	−
	2	lung	NC + F	20	26	+	3	+	0	−
	3	lung	NC + F	32	0	−	3	indeterminate	0	−
	4	lung	NC	20	0	−	0	−	0	−
	5	lung	NC	40	0	−	2	indeterminate	0	−
	6	lung	NC	40	4	indeterminate	0	−	0	−
	7	lung	NC + F	20	1	indeterminate	1	indeterminate	0	−
	8	lung	NC	20	0	−				
	9	lung	NC	20	0	−	0	−	0	−
	10	lung	NC	20	6	+	1	indeterminate	0	−
	11	lung	NC	28	5	+	3	+	0	−
	12	LN	NC	32	9	+			0	−
	13	LN	NC	28	7	+	3	+	0	−
	14	LN	NC	28	2	indeterminate	4	+		
	15	LN	NC	36	0	−	3	indeterminate	0	−
	16	LN	NC	28	5	+	3	+	0	−
	17	LN	NC	16	0	−	0	−	0	−
	18	LN	NC	16	0	−	1	indeterminate	0	−

[a]CAS, caseous granulomatous inflammation; NC, noncaseating granulomatous inflammation; diff-GC, diffuse granulomatous inflammation with giant cells; Int, cellular interstitial infiltrate; F, fibrosis.
[b]Number of high power fields (400×) viewed for analysis.
[c]Number of focal collections of ISH staining (positive signal).
[d]Negative, <0.5 focal collections per 10 high power fields examined; indeterminate, 0.5–1.0 focal collections per 10 high power fields examined; positive, >1.0 focal collections per 10 high power fields examined.

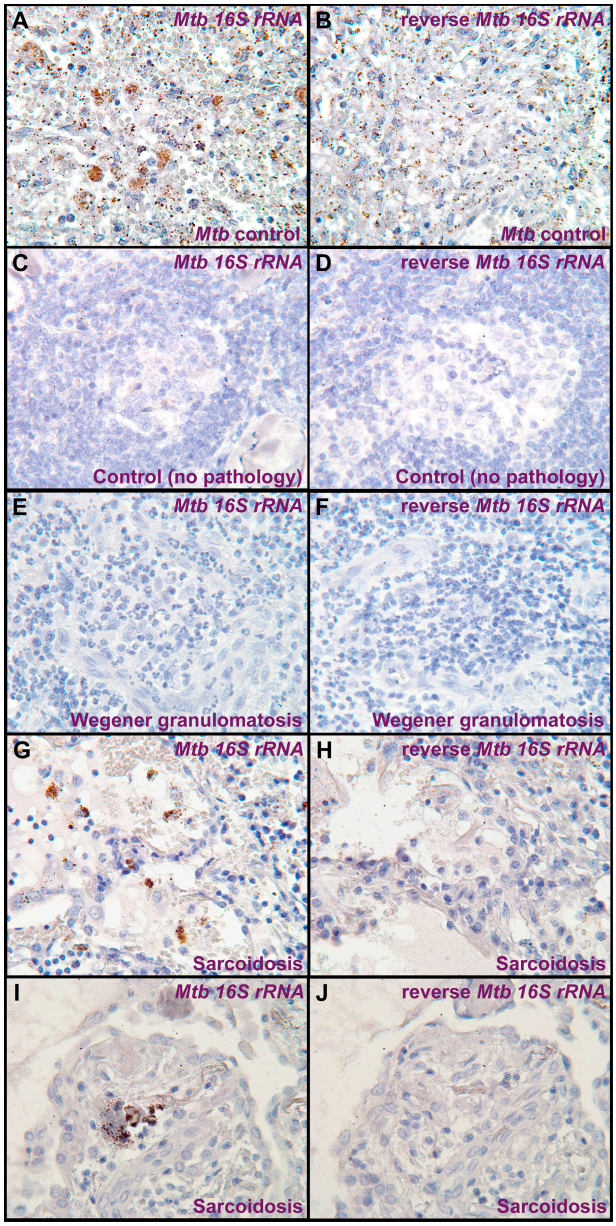

Figure 5. Cellular localization of *Mtb 16S rRNA* DNA by ISH. Shown are representative photomicrographs from biopsies of *Mtb*-infected tissue (A and B), normal controls (no pathology; C and D), Wegener granulomatosis (E and F), and sarcoidosis tissues (G–J). Tissue sections were hybridized with or without DIG-labeled probes, detected with anti-DIG $F(ab')_2$ fragments conjugated with alkaline phosphatase, and developed with Vector Red substrate. *Mtb*-infected tissue (A) and sarcoidosis samples (G and I) demonstrated focal collections of *Mtb 16S rRNA* DNA that were not seen in Wegener granulomatosis (E) nor in nongranulomatous control tissues (C). All tissues were negative using reverse *Mtb 16S rRNA* probes.

in all PPD^+ subjects (10 of 10), in 6 of 11 (55%) PPD^- controls, and in 17 of 25 (68%) sarcoidosis patients (group comparison, $P = 0.0129$; PPD^+ vs. sarcoidosis, $P = 0.0363$; PPD^+ vs. PPD^-, $P = 0.0351$; Fig. 6 B and Table III). Within the sarcoidosis group, all 12 $mKatG^+$ sera also bound to mHsp65, suggesting the presence of reactivity to mycobacterial antigens other than mKatG in this subset of patients. The proportion of sarcoidosis patients with reactivity to mHsp65 but not mKatG (6 of 12 [50%]) was not statistically different from PPD^- controls ($P > 0.9$), suggesting a nondisease-specific reactivity or cross-reactivity to mHsp65 in these patients.

DISCUSSION

The studies presented here demonstrate the existence of a small number of protease-resistant, poorly soluble antigens in sarcoidosis tissues that are targets of an adaptive T cell–dependent IgG response in patients with this disease. Sarcoidosis-specific target antigens were discriminated from antigens in control tissues by using a limited proteomic approach that preferentially concentrated proteins resistant to protease digestion in neutral detergent, or by selecting for poorly soluble protein aggregates using a moderately denaturing detergent extraction method. The fact that these biochemical treatments are known to preserve and concentrate the in vivo granuloma-inducing activity of sarcoidosis tissue homogenates enhances the probability that these specific tissue antigens are relevant to the disease pathogenesis. More importantly, we identified one of these candidate antigenic targets to be derived from the mycobacterial KatG protein. This identification was initially made by MALDI-TOF mass spectrometric peptide fingerprinting but was critically verified using specific anti-mKatG mAbs and immunoblot analysis. Further support for these findings was provided by the detection of *mKatG* DNA using ISH techniques in a subset of sarcoidosis tissues. Together, these results provide evidence that poorly soluble protein aggregates containing mKatG are present in a subset of sarcoidosis tissues, representing a potential target for local adaptive immune responses.

The mycobacterial catalase–peroxidase protein encoded by *katG* is found in most mycobacterial species and is a highly expressed protein in *Mtb* and *M. smegmatis* (unpublished data). KatG is an important virulence factor that provides protection from the deleterious effects of peroxide, allowing survival of mycobacterial organisms inside macrophages (23). Isoniazid, a frontline antimycobacterial agent, requires conversion to its active form by KatG before it has antimycobacterial effects (24, 25). Total or partial deletion of *katG* as well as mutations that inactivate it lead to isoniazid resistance (24, 26, 27). Although the crystallographic structure of mKatG has not yet been reported, there is strong evidence that the enzyme is a homodimer in its native form, with mutant forms displaying differences in electrophoretic mobility and enzymatic function (21, 22).

The presence of KatG protein and DNA from *Mtb* or possibly *M. smegmatis* in sarcoidosis tissues indicates that previous exposure to these organisms or closely related mycobacterial organisms occurs in a subset of patients with sarcoidosis. The results of this study follow previous reports that remnants of mycobacterial organisms are present in sarcoidosis tissues assessed by biochemical or immunohistochemical techniques (28, 29). In one study, both cross-reactive and

Table IV. Circulating IgG responses to recombinant mKatG and mHsp65 in sarcoidosis patients and PPD$^-$ and PPD$^+$ control subjects

	mKatG		mHsp65			mKatG		mHsp65
	80 kD	60 kD	65 kD	CXR stage[a]		80 kD	60 kD	65 kD
Sarcoidosis					**PPD$^-$**			
S1	+[b]	−	+	2	N1	−	−	−
S2	−	−	−	2	N2	−	−	−
S3	−	+	+	1	N3	−	−	−
S4	−	−	−	2	N4	−	−	+
S5	−	−	−	2	N5	−	−	+
S6	−	−	+	1	N6	−	−	−
S7	−	−	−	2	N7	−	−	−
S8	−	−	−	2	N8	−	−	+
S9	−	+	+	2	N9	−	−	+
S10	−	+	+	2	N10	−	−	+
S11	−	+	−	1	N11	−	−	+
S12	−	−	+	1	**PPD$^+$**			
S13	−	+	+	1	P1	++	++	+
S14	−	+	+	1	P2	+	−	+
S15	−	−	−	3	P3	−	−	+
S16	−	−	+	1	P4	−	−	+
S17	+	+	+	2	P5	−	−	+
S18	−	+	+	3	P6	−	−	+
S19	++[c]	+	+	0	P7	−	−	+
S20	++	+	+	2	P8	+	−	+
S21	+	+	+	2	P9	−	−	+
S22	−	−	+	1	P10	+	−	+
S23	−	−	−	1				
S24	−	−	+	0				
S25	−	−	+	1				

[a]Stage 0, normal chest radiograph; stage 1, bilateral hilar adenopathy; stage 2, bilateral hilar adenopathy plus interstitial infiltrates; stage 3, pulmonary infiltrates only (no hilar adenopathy).
[b]Titer 1:500.
[c]Titer .1:1,000.

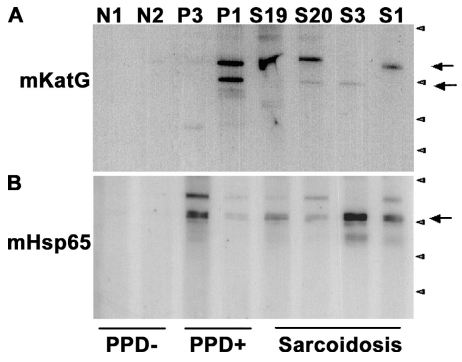

Figure 6. Circulating IgG from patients with sarcoidosis binds to recombinant mKatG and mHsp65 protein. Protein immunoblots with recombinant mKatG (A) or mHsp65 (B) were analyzed with IgG purified from the sera of healthy PPD$^-$ (N), PPD$^+$ (P) subjects or sarcoidosis (S) patients corresponding to Table IV. Arrowheads demark migration of mol wt markers (top to bottom: 188, 62, 49, and 38 kD). Arrows demark ~80- and ~60-kD antigenic bands reactive to mKatG or a 65-kD band reactive to mHsp65.

species-specific antigenic determinants from *Mtb* proteins and cell wall products were found in Schaumann bodies in sarcoidosis tissue by immunohistochemistry (29). Multiple PCR-based studies report widely varying results with traces of mycobacterial nucleic acids detected in 0–80% of sarcoidosis tissues (30–34). In a recently reported study, Drake et al. (35) reported detecting mycobacterial *rRNA* or *rpoB* sequences in 60% of sarcoidosis tissues but in none of the control tissues. Consistent with these results, we detected *mKatG* and *Mtb. 16S rRNA* DNA in a subset of sarcoidosis tissues using ISH techniques. These data strengthened the initial findings from our limited proteomic approach and together provided new evidence for the hypothesis that exposure to mycobacterial organisms may trigger sarcoidosis in a subset of patients (36).

Additional support for a mycobacterial etiology of sarcoidosis is provided by our finding that the proportion of sarcoidosis patients with circulating antibodies to mKatG was similar to PPD$^+$ subjects with either previous wild-type ex-

posure to *Mtb* or previous Bacille Calmette-Guerin (BCG) vaccination. This proportion was significantly higher than in PPD^- subjects, suggesting that mKatG is a specific immunologic target common to a subset of PPD^+ individuals and sarcoidosis patients. This conclusion is bolstered by our finding that all sarcoidosis patients with circulating antibodies to mKatG also had circulating antibodies directed against mHsp65, indicating that these patients have serologic reactivity to mycobacterial antigens that extend beyond mKatG. The proportion of sarcoidosis patients with reactivity to mHsp65 but not mKatG was similar to that found in PPD^- controls, consistent with a nondisease-specific immunologic reactivity or cross-reactivity to mHsp65 in these subjects as has been reported previously (37, 38). Within the PPD^+ group, serologic reactivity to mHsp65 was more frequent than reactivity to mKatG, suggesting that mHsp65 might be a more dominant immunologic target than mKatG in BCG-vaccinated individuals or those with latent *Mtb*. Whether differences in the immune responses to these specific mycobacterial proteins play a role in determining clinical outcomes after mycobacterial exposure remains unknown. Given the lack of correlation between mKatG reactivity and clinical course in our series, it appears likely that the presence of anti-mKatG IgG responses does not determine clinical outcome by itself in sarcoidosis.

The presence of mycobacterial proteins in sarcoidosis tissues might be relevant to long-term immunologic stimulation as a result of either antigen persistence or from the development of autoimmunity by molecular mimicry (39–41). Our findings that mKatG is often present in sarcoidosis tissues at time of diagnosis and might be associated with anti-mKatG responses suggests that antigen persistence plays a role by promoting local adaptive immune responses associated with active granuloma formation in sarcoidosis. Because mKatG is not known to be inherently resistant to protease digestion, our findings suggest that mKatG is denatured in vivo and complexed with poorly soluble tissue components that provide relative protection against protease attack. These protein/tissue aggregates may serve as an antigenic reservoir for eventual degradation by dendritic cells or other mononuclear phagocytes with subsequent antigen presentation of derived peptides (42, 43). The potential for mKatG to serve as a target antigen in sarcoidosis is supported by our preliminary studies that mKatG complexed to Sephadex beads strongly induces granuloma formation in a previously described rodent model of granulomatous inflammation (unpublished data and references 10, 44, and 45).

Although this study identified mKatG as one target of the adaptive immune response in sarcoidosis, other poorly soluble, protease-resistant tissue antigens have not yet been identified. Because mKatG was found in only a subset of tissues, it is plausible, if not likely, that other microbial antigens or endogenous proteins as autoantigens promote local adaptive immune responses as part of the pathogenic granulomatous inflammation in other groups of sarcoidosis patients. The identification of these other tissue antigens has been impeded by the small amounts of tissue that are obtained during standard biopsy procedures and the resulting trace amounts of protein antigens isolated in a mixture with other tissue components. Despite the inherent difficulties in determining the identity of these tissue antigens, results from this study suggest that there might be only a small number of tissue antigens that are specific targets of an adaptive humoral response associated with granulomatous inflammation in sarcoidosis. More generally, the identification of mKatG as a target tissue antigen supports the concept that granulomas in sarcoidosis contain pathobiologically relevant antigens capable of reconstructing the natural history of sarcoidosis. Identification of other disease-specific tissue antigens is likely to provide further insight into the etiopathogenesis of sarcoidosis and demonstrate the feasibility of using this type of limited proteomic approach to detect pathogenic antigens in other human granulomatous diseases.

MATERIALS AND METHODS

Patient populations. Tissue specimens were obtained from two sources. First, portions of tissue biopsies from patients with suspected sarcoidosis who were undergoing diagnostic procedures were prospectively collected with patient consent under an institutional review board (IRB)-approved protocol if part of the biopsy sample was not needed for clinical purposes. Second, archived surgical specimens from patients with confirmed sarcoidosis or from control groups from The Johns Hopkins Hospital or Mount Sinai Medical Center were obtained with IRB approval within institutional guidelines for the use of archived tissues. All tissues were processed similarly after surgical biopsy with unused fresh frozen or fixed, paraffin-embedded tissue used for research only after confirmation of a clinical and pathologic diagnosis. Sarcoidosis tissues were from patients with a final diagnosis of sarcoidosis based on clinical criteria and biopsy showing typical noncaseating epithelioid granulomas without evidence of bacterial, mycobacterial, or fungal organisms using standard special stains (Kinyoun's acid fast, auramine rhodamine, and Gomori's methanamine silver stains) or culture in accordance with consensus criteria (1). Control lymph node tissues were from patients who had undergone surgical biopsy or resection to exclude malignancy or evaluate lymphadenopathy of unknown cause. In all but two cases, the samples showed no evidence of malignancy, infection, or granuloma. Two lymph nodes demonstrated follicular hyperplasia that were consistent with a clinical diagnosis of an autoimmune disease. Control lung tissues were from patients with biopsy-proven Wegener granulomatosis, usual interstitial pneumonia, or without pathology (no evidence of malignancy, infection, or granuloma) from patients who had undergone biopsy to exclude malignancy. Control spleen tissues were obtained from splenectomy samples from patients who had undergone surgery for abdominal malignancy.

Peripheral blood for sera was obtained from patients with biopsy-proven sarcoidosis, PPD^- healthy controls, and PPD^+ subjects. All patients were recruited under IRB-approved protocols. A diagnosis of sarcoidosis was based on a compatible clinical history and biopsy according to consensus criteria (1). 6 patients had clinical evidence for pulmonary involvement only and 19 patients had clinical evidence of extrapulmonary disease with or without pulmonary involvement, consistent with published criteria (1, 46). Chest radiograph staging was determined according to international convention (1). Based on clinical presentation and chest radiograph, all patients had active sarcoidosis at time of phlebotomy (1).

The PPD^+ group of control subjects either had a history of BCG vaccination or had known or presumed prior infection with *Mtb*. Standard PPD skin testing using intradermal injection of 5 tuberculin units of PPD (Tubersol; Aventis Pasteur) was performed to confirm the status of self-reported PPD^+ volunteers (47). Responses to PPD were assessed as largest diameter of induration present 48 h after injection. For the purposes of this study, in-

duration of ≥10 mm at the time of follow-up examination was considered a positive skin test response.

Reagents. TX100, *n*-laural sarkosine (sarkosyl), micrococcal nuclease, and PK were purchased from Sigma-Aldrich and were of the highest quality available. Recombinant Hsp65 from batch number MA-11A was obtained from M. Singh (World Health Organization [WHO], Braunschweig, Germany) from the WHO Recombinant Protein Bank with financial support from the UNDP/World Bank/WHO Special Program for Research and Training in Tropical Diseases.

mAb IT57, reactive to mKatG, was obtained from Colorado State University and was produced through funds from the National Institutes of Health (NIH), National Institute of Allergy and Infectious Diseases (contract N0-AI-75320 entitled "Tuberculosis Research Materials and Vaccine Testing"; reference 20).

TX100 extraction. Tissues were processed according to protocols similar to ones that were previously reported to preserve and concentrate the in vivo granuloma-inducing activity of sarcoidosis tissue homogenates (13, 17, 18). In brief, samples of frozen lymph node, spleen, or lung ranging from 0.1–2 g total weight were homogenized at a ratio of 1:10 in PBS, pH 7.4, using a polytron with five to six 10-s bursts on medium speed. The suspension was centrifuged at 500 *g* for 10 min, and the supernatant was saved. The pellet was resuspended in PBS and the homogenization procedure was repeated. The supernatants were pooled and centrifuged at 22,000 *g* (16,000 rpm; T-30 rotor) for 40 min. The pellets were resuspended in PBS, centrifuged at 22,000 *g* for 30 min, washed in PBS, resuspended, sonicated twice for ∼1 min each, and forced through 100-wire mesh. The suspension was again sonicated, centrifuged at 22,000 *g* for 30 min, and the supernatant was removed to collect the pellet (P22). The pellet was stored overnight at 4°C and then resuspended in PBS and diluted to a concentration of ∼100 mg/ml. TX100 (a final concentration of 2%) was added to 400 μl of this suspension in a microfuge tube, and the suspension was shaken for 2 h at 37°C. 10 U/ml micrococcal nuclease was added and the suspension was shaken for 3 h at 37°C. The suspension was divided into two 200-μl aliquots, one of which received 100 μg/ml PK. Both aliquots were rotated for 16 h at room temperature, and then the reaction was stopped by adding 0.2 mM PMSF to each aliquot. The aliquots were extracted with a 1:1 solution of 2:1 chloroform/methanol by continuous rotation for 30 min and spun in a microfuge tube at 12,000 rpm. The pellets were washed in ice-cold 80% methanol for 30 min, spun for 30 min at 12,000 rpm, and the pellets were washed again in ice-cold 80% ethanol. After a 30-min centrifugation in a microfuge at 12,000 rpm, the resultant pellet was resuspended in 170 μl 8 M urea plus 0.1 M β-mercaptoethanol in 0.1 M sodium phosphate Tris buffer, pH 7.4, plus 0.2 mM PMSF for 20 h at 4°C. After centrifugation in a microfuge at 12,000 rpm for 30 min, the supernatant was collected, precipitated with nine volumes of 1:2 chloroform/methanol for 30 min on ice, spun at 12,000 rpm, and then washed in ice-cold methanol and ethanol as detailed above. The final pellets were either analyzed directly by SDS-PAGE or lyophilized and stored at −80°C for later analysis.

Sarkosyl extraction. To enrich for poorly soluble protein aggregates, a moderately denaturing detergent extraction was used that previously had been used to enrich for prion protein aggregates (19). Tissue samples of 1.7–5 g total weight were homogenized as described above and processed to yield PBS-insoluble tissue pellets (P22), which were stored at −80°C until use. The pellets (P_{22}) were thawed and resuspended in 12–24 ml of 1% sarkosyl in PBS at a concentration of ∼100 mg/ml, ultrasonicated intermittently for 1 min followed by mixing for 1 h, and then centrifuged at 22,000 *g* for 20 min. The resultant supernatant (S22) was centrifuged at 215,000 *g* (46,000 rpm with a Ti60 rotor) for 2 h. The pellet (P215) was resuspended in buffer (1% sarkosyl, 10% NaCl, 50 mM Tris, pH 7.4) and spun at 215,000 *g* for 2.5 h. The pellet was collected, resuspended in the same buffer (1% sarkosyl, 10% NaCl, 50 mM Tris, pH 7.4), and stirred overnight at 37°C. The suspension was transferred to a microfuge tube, spun 20 min at 12,000 rpm, and the pellet (P1) was resuspended in 1 ml buffer (0.2% sarkosyl, 10% NaCl, 50 mM Tris, pH 7.4) with shaking at 37°C for 1 h. The pellets (P2) were resuspended in 1 ml buffer (0.1% sarkosyl in 50 mM Tris, pH 7.4) and shaken at 37°C for 1 h. The samples were spun for 20 min in a microfuge at 12,000 rpm and the process was repeated. The resulting pellet was resuspended in a microfuge tube in 8 M urea, 0.1 M sodium phosphate, Tris 7.4 buffer plus 0.1 M β-mercaptoethanol, and gently shaken overnight at 4°C. The samples were then spun in a microfuge at 12,000 rpm, and the supernatant was precipitated with 1:1 chloroform/methanol (1:2) followed by washing the pellet in 80% ethanol as detailed above to yield the final pellet (Pe). The pellets were either used directly in gel electrophoresis or lyophilized and stored at 4°C for later analysis.

Protein immunoblot. Total protein content was analyzed by the bicinchroninic acid method for colorimetric detection and quantification (BCA Protein Assay Kit; Pierce Chemical Co.). Protein samples were analyzed by gel electrophoresis using either 10–20% Tris-HCl SDS-PAGE (Bio-Rad Laboratories) or 4–12% NuPAGE Bis-Tris gels (Novex) according to the manufacturer's recommendations. Gels were stained with either a silver stain or Coomassie Brilliant Blue colloidal stain (Sigma-Aldrich). Gels were electroblotted onto nitrocellulose membranes (Schleicher and Schuell) according to manufacturer's recommendations. Immunoblots were preincubated with nonfat dried milk dissolved in TTBS (2% dry milk/0.1% Tween 20 in PBS), and then primary antibodies were added. Protein immunoblots were probed with either total IgG or $F(ab')_2$ fragments derived from pooled sera from one of three sets of five to six individual sarcoidosis patients or two sets of control sera. Total IgG was purified by Protein A affinity Pak (Pierce Chemical Co.) chromatography according to the manufacturer's recommendations. $F(ab')_2$ fragments were derived from total IgG by using the ImmunoPure $F(ab')_2$ preparation kit (Pierce Chemical Co.) with immobilized pepsin bound to beaded agarose, according to the manufacturer's recommendations. Secondary antibody reagents were anti–human Fab or Fcγ (Sigma-Aldrich) linked to horseradish peroxidase (HRP) detected with the ECL system (Amersham Biosciences). Immunoblots were stripped of their primary antibody by agitating in stripping solution (100 mM 2-mecaptoethanol, 2% SDS, 62.5 mM Tris-HCl, pH 6.7) for 30 min at 50°C or by Restore Western Blot stripping buffer (Pierce Chemical Co.) according to the manufacturer's recommendations.

MALDI-TOF mass spectroscopy. Samples were run on 4–12% NuPAGE Bis-Tris gels (Novex) and stained with a Coomassie Brilliant Blue colloidal stain. Protein bands were excised based on migration of mol wt markers. Proteins in the excised bands were digested with trypsin in situ, and the resulting peptides were extracted, precipitated under low and high salt conditions, and analyzed by MALDI-TOF mass spectrometry as described previously (48, 49). In brief, gel slices were placed into an Eppendorf tube with a ratio of 1:1 (vol/vol) acetonitrile/25 mM ammonium bicarbonate added for 30 min or until the majority of blue dye was removed. The gel slice was dried completely under vacuum. 2 μL trypsin solution (0.1 μg/μL in 1% acetic acid) and 25 μl of buffer (25 mM ammonium bicarbonate) were added, and the reaction mixture was incubated at 37°C overnight. The tryptic fragments were extracted twice from the gel by adding 30 μl of 1:1 (vol/vol) acetonitrile/water, 5% trifluoroacetic acid. The extraction mixture was dried under a vacuum to an approximate volume of 5 μL. The reaction mixture (0.3 μL) was deposited onto a stainless steel sample probe followed by 0.3 μl of saturated α-cyano-4-hydroxycinnamic acid matrix (1:1 vol/vol ethanol/water). Mass spectra were acquired on a Kratos Kompact MALDI 4 time of flight mass spectrometer equipped with a nitrogen laser (337 nm). Mass spectra were calculated using trypsin autolysis peaks or internal standards.

The peptide mass fingerprint was analyzed by protein database sequence searching using the OWL database and the MOWSE-based search engine using Protein Prospector at the University of California, San Francisco web site (http://prospector.ucsf.edu) or the Mascot search engine (Matrix Science, Ltd.: http://www.matrixscience.com; reference 50).

Overexpression and purification of mKatG. mKatG protein was overexpressed from the plasmid construct pYZ56, which contained the *katG* gene in a 2.9-kD EcoRV–KpnI fragment in pUC19 vector (24). The KatG protein forms a fusion protein with 22 amino acids of the *lacZ* gene, and the overexpression was driven by the *lacZ* promoter on the pUC19. The pYZ56 construct was transformed into the *E. coli* catalase mutant UM2 and the transformant was grown in LB medium containing 50 μg/ml ampicillin overnight (24). Protein extracts were prepared by sonication on ice, and the purification of the KatG protein was performed as described by Johnsson et al. (51). For protein immunoblots, recombinant mKatG was precipitated in 80% ethanol overnight, and the mixture was centrifuged in a microfuge at 12,000 rpm for 20 min. The pellet was then resuspended in loading buffer and used in protein immunoblot procedures.

Bacterial extract preparation. Bacterial and mycobacterial cultures were grown to early stationary phase, centrifuged, and cell pellets were washed twice with PBS. The cells were then resuspended in PBS, and soluble protein extracts were prepared by sonication followed by centrifugation.

ISH with TSA. To detect the presence of *mkatG* DNA in paraffin-embedded archival biopsy tissue samples, we performed ISH with TSA using a manufacturer's reagents and protocol (GenPoint kit K0620; DakoCytomation) modified for use with digoxigenin (DIG)-tailed probes (52–54). The presence of mycobacterial DNA in tissue samples was also evaluated using ISH without TSA using *Mtb 16S rRNA* probes.

Oligonucleotide probes specific for *mkatG* (gcccaaggtatctcgcaacg; GenBank accession no. 488449) or *Mtb16S rRNA* (accggcttttaaggattcgctta; GenBank accession no. 44689) were designed using the online NCBI BLAST tool (Blast2seq). Reverse sequence oligonucleotides from *mkatG* or *Mtb 16S rRNA* probes or *H. pylori 16S rRNA* (ggacataggctgatctcttagc; GenBank accession no. 21314562) were used as controls. Probes were 3′ end labeled with DIG-11-dUTP (DIG oligonucleotide tailing kit; Roche Applied Science) and diluted with hybridization buffer (S3304; DakoCytomation) to a final concentration of 100 nM.

ISH-TSA was performed with 8-μm slides that were deparaffinized, treated with target retrieval solution (S1700; DakoCytomation) in a steamer for 20 min, and digested with PK (S3004; DakoCytomation) diluted at 1:2,500 for 5 min. Background peroxidase activity was quenched with 0.3% hydrogen peroxide in methanol, and the slides were air-dried. 20–40 μl of probe mixture was placed onto sections, the slides were coverslipped, heated to 97°C for 5 min, and then immediately placed into a humidified oven and incubated for 18 h at 56 (*mkatG* probes), 58 (*Mtb 16S rRNA* probes), or 37°C (*H. pylori 16s rRNA* probes). Sections were rinsed with PBS with 0.05% Tween-20, washed twice with stringent wash solution (GenPoint kit; DakoCytomation) at the appropriate temperature (56°C for *mkatG*, 63°C for *Mtb 16S rRNA*, or 45°C for *H. pylori 16S rRNA*), and then incubated with rabbit $F(ab')_2$ anti-DIG antibodies conjugated to HRP (DakoCytomation). Signal amplification was performed by incubation with biotinylated tyramine. After a final wash, sections were incubated with streptavidin conjugated to HRP. Hybridized sections were developed with a DAB chromogen solution followed by counterstaining with hematoxylin. ISH without TSA was performed by incubation with sheep $F(ab')_2$ anti-DIG antibodies conjugated with alkaline phosphatase (Roche). After a final wash, sections were developed with Vector Red substrate (Vector Laboratories) and counterstained with hematoxylin.

Tissue sections were examined under low (100×) and high power (400×) light microscopy. Positive control tissues included two archived biopsy samples from patients with culture-positive *Mtb* infection and commercially available slides with mycobacterial infection approved for clinical laboratory use (Histology Control Systems, Inc. and Sigma-Aldrich). All areas involved with inflammation (*Mtb*, sarcoidosis, Wegener granulomatosis, and usual interstitial pneumonia) or nondiseased areas of no-pathology control tissues were examined for focal collections of stain (a minimum of 10 high power fields). Based on analyses of reverse probe controls and known mycobacterial infected control tissues, the following criteria were established: the presence of <0.5 stained foci per 10 high power fields was interpreted as "negative"; the presence of 0.5–1.0 stained foci per 10 high power fields was read as "indeterminate"; and the presence of >1.0 stained foci per 10 high power fields was read as "positive."

Statistical analysis. Comparisons were performed by Chi-square analysis with the two-tailed Fisher's exact test using JMP Statistical Discovery Software, version 5 (SAS Institute, Inc.). A probability value of $P < 0.05$ was considered significant.

Online supplemental material. Tables S1 and S2 provide summaries of potential peptide matches for *Mtb* topoisomerase I and *M. smegmatis* KatG from MALDI-TOF mass spectrometry of sarcoidosis tissues. Fig. S1 shows a representative protein immunoblot of recombinant mKatG and sonicated cell-free extracts of *Mtb*, *M. smegmatis*, *M. chelonei*, *H. pylori*, and *E. coli* using the anti-mKatG IT57 mAb. Tables S1, S2, and Fig. S1 are available at http://www.jem.org/cgi/content/full/jem.20040429/DC1.

We acknowledge the expert technical assistance of Shannon Heine.

This work was supported in part by NIH grants HL-54658 (to D.R. Moller), HL-68019 (to D.R. Moller), and GM-54882 (to R.J. Cotter), the Life and Breath Foundation, and the Hospital for the Consumptives of Maryland (Eudowood).

The authors have no conflicting financial interests.

Submitted: 5 March 2004
Accepted: 6 January 2005

REFERENCES

1. Statement on sarcoidosis. 1999. Joint Statement of the American Thoracic Society (ATS), the European Respiratory Society (ERS) and the World Association of Sarcoidosis and Other Granulomatous Disorders (WASOG) adopted by the ATS Board of Directors and by the ERS Executive Committee, February 1999. *Am. J. Respir. Crit. Care Med.* 160:736–755.
2. Robinson, B.W., T.L. McLemore, and R.G. Crystal. 1985. Gamma interferon is spontaneously released by alveolar macrophages and lung T-lymphocytes in patients with pulmonary sarcoidosis. *J. Clin. Invest.* 75:1488–1495.
3. Moller, D.R., J.D. Forman, M.C. Liu, P.W. Noble, B.M. Greenlee, P. Vyas, D.A. Holden, J.M. Forrester, A. Lazarus, M. Wysocka, and G. Trinchieri. 1996. Enhanced expression of IL-12 associated with Th1 cytokine profiles in active pulmonary sarcoidosis. *J. Immunol.* 145: 4952–4960.
4. Greene, C.M., G. Meachery, C.C. Taggart, C.P. Rooney, R. Coakley, S.J. O'Neill, and N.G. McElvaney. 2000. Role of IL-18 in CD4+ T lymphocyte activation in sarcoidosis. *J. Immunol.* 165:4718–4724.
5. Forman, J.D., J.T. Klein, R.F. Silver, M.C. Liu, B.M. Greenlee, and D.R. Moller. 1994. Selective activation and accumulation of oligoclonal V beta-specific T-cells in active pulmonary sarcoidosis. *J. Clin. Invest.* 94:1533–1542.
6. Grunewald, J., C.H. Janson, A. Eklund, M. Ohm, O. Olerup, U. Persson, and H. Wigzell. 1993. Restricted Va2.3 gene usage by CD4+ T lymphocytes in bronchoalveolar lavage fluid from sarcoidosis patients correlates with HLA-DR3. *Eur. J. Immunol.* 22:129–135.
7. Forrester, J.M., Y. Wang, N. Ricalton, J.E. Fitzgerald, J. Loveless, L.S. Newman, T.E. King, and B.L. Kotzin. TCR expression of activated T cell clones in the lungs of patients with pulmonary sarcoidosis. 1994. *J. Immunol.* 153:4291–4302.
8. Selroos, O., M. Klockars, R. Kekomaki, K. Pentinen, P. Lindstrom, and O. Wagner. 1980. Circulating immune complexes in sarcoidosis. *J. Clin. Lab. Immunol.* 3:129–132.
9. Scott, P., E. Pearce, A.W. Cheever, R.L. Coffman, and A. Sher. 1989. Role of cytokines and CD4+ T-cell subsets in the regulation of parasite immunity and disease. *Immunol. Rev.* 112:161–182.
10. Kunkel, S.L., N.W. Lukacs, R.M. Strieter, and S.W. Chensue. 1996. Th1 and Th2 responses regulate experimental lung granuloma development. *Sarcoidosis Vasc. Diffuse Lung Dis.* 13:120–128.
11. Siltzbach, L.E. 1961. The Kveim test in sarcoidosis: a study of 750 patients. *J. Am. Med. Assoc.* 178: 476–482.

12. Teirstein, A.S. The Kveim test after Siltzbach. 1986. *Ann. NY Aca. Sci.* 465:744–746.
13. Munro, C.S., and D.N. Mitchell. 1987. The Kveim response: still useful, still a puzzle. *Thorax.* 42:321–331.
14. Sullivan, L., S. Sano, C. Pirmez, P. Salgame, C. Mueller, F. Hofman, K. Uyemura, T.H. Rea, B.R. Bloom, and R.L. Modlin. 1991. Expression of adhesion molecules in leprosy lesions. *Infect. Immun.* 59:4154–4160.
15. Favez, G., and P. Leuenberger. 1982. Significance of circulating antibodies directed against the Kveim suspension demonstrated in patients with sarcoidosis. *J. Clin. Lab. Immunol.* 9:87–91.
16. Klein, J.T., T.D. Horn, J.D. Forman, R.F. Silver, A.S. Teirstein, and D.R. Moller. 1994. Selection of oligoclonal V beta-specific T-cells in the intradermal response to Kveim-Siltzbach reagent in individuals with sarcoidosis. *J. Immunol.* 154:1450–1460.
17. Chase, M.W., and L.E. Siltzbach. 1967. Concentration of the active principle responsible for the Kveim reaction. *La Sarcoidose.* 196:150–160.
18. Lyons, D., S. Donald, D. Mitchell, and G. Asherson. 1992. Chemical inactivation of the Kveim reagent. *Respiration (Herrlisheim).* 59:22–26.
19. Hilmert, H., and H. Diringer. 1984. A rapid and efficient method to enrich SAF-protein from scrapie brains of hamsters. *Biosci. Rep.* 4:165–170.
20. Sonnenberg, M., and J. Belisle. 1997. Definition of *Mycobacterium tuberculosis* culture filtrate proteins by two dimensional polyacrylamide gel electrophoresis, N-terminal amino acid sequencing, and electrospray mass spectrometry. *Infect. Immun.* 65:4515–4524.
21. Nagy, J.M., A.E. Cass, and K.A. Brown. 1997. Purification and characterization of recombinant catalase-peroxidase, which confers isoniazid sensitivity in *Mycobacterium tuberculosis*. *J. Biol. Chem.* 272:31265–31271.
22. DeVito, J.A., and S. Morris. 2003. Exploring the structure and function of the mycobacterial KatG protein using trans-dominant mutants. *Antimicrob. Agents Chemother.* 47:188–195.
23. Manca, C., S. Paul, C.E. Barry, V.H. Freedman, and G. Kaplan. 1999. *Mycobacterium tuberculosis* catalase and peroxidase activities and resistance to oxidative killing in human monocytes in vitro. *Infect. Immun.* 67:74–79.
24. Zhang, Y., B. Heym, B. Allen, D. Young, and S. Cole. 1992. The catalase-peroxidase gene and isoniazid resistance of *Mycobacterium tuberculosis*. *Nature.* 358:591–593.
25. Zhang, Y., T. Garbe, and D. Young. 1993. Transformation with katG restores isoniazid sensitivity in *Mycobacterium tuberculosis* isolates resistant to a range of drug concentrations. *Mol. Microbiol.* 8: 521–524.
26. Zhang, Y., and D. Young. 1994. Strain variation in the katG region of *Mycobacterium tuberculosis*. *Mol. Microbiol.* 14:301–308.
27. Cockerill, F.R., III, J.R. Uhl, Z. Temesgen, V. Zhang, L. Stockman, G.D. Roberts, D.L. Williams, and B.C. Kline. 1995. Rapid identification of a point mutation of the *Mycobacterium tuberculosis* catalase-peroxidase gene (*katG*) associated with isoniazid resistance. *J. Infect. Dis.* 171:240–245.
28. Hanngren, A., G. Oedham, A. Eklund, S. Hoffner, N. Stjernberg, and G. Westerdahl. 1987. Tuberculostearic acid in lymph nodes from patients with sarcoidosis. *Sarcoidosis.* 4:101–104.
29. Ang, S.C., and E.A. Moscovic. 1996. Cross-reactive and species specific *Mycobacterium tuberculosis* antigens in the immunoprofile of Schaumann bodies: a major clue to the etiology of sarcoidosis. *Histol. Histopathol.* 11:125–134.
30. Mangiapan, G., and A.J. Hance. 1995. Mycobacteria and sarcoidosis: an overview and summary of recent molecular biological data. *Sarcoidosis.* 12:20–37.
31. Bocart, D., D. Lecossier, A. De Lassence, D. Valelyre, J. Battesti, and A.J. Hance. 1992. A search for Mycobacterial DNA in granulomatous tissues from patients with sarcoidosis using the polymerase chain reaction. *Am. Rev. Respir. Dis.* 145:1142–1148.
32. Popper, H.H., E. Winter, and G. Hofler. 1994. DNA of *Mycobacterium tuberculosis* in formalin-fixed, paraffin-embedded tissue in tuberculosis and sarcoidosis detected by polymerase chain reaction. *Am. J. Clin. Pathol.* 101:738–741.
33. Ishige, I., Y. Usui, T. Takemura, and Y. Eishi. 1999. Quantitative PCR of mycobacterial and propionibacterial DNA in lymph nodes of Japanese patients with sarcoidosis. *Lancet.* 354:120–123.
34. Richter, E., Y.P. Kataria, G. Zissel, J. Homolka, M. Schlaak, and J. Muller-Quernheim. 1999. Analysis of the Kveim-Siltzbach test reagent for bacterial DNA. *Am. J. Respir. Crit. Care Med.* 159:1981–1984.
35. Drake, W.P., Z. Pei, D.T. Pride, R.D. Collins, T.L. Cover, and M.J. Blaser. 2002. Molecular analysis of sarcoidosis tissues for mycobacterium species DNA. *Emerg. Infect. Dis.* 11:1334–1341.
36. du Bois, R.M., N. Goh, D. McGrath, and P. Cullinan. 2003. Is there a role for microorganisms in the pathogenesis of sarcoidosis? *J. Intern. Med.* 253:4–17.
37. Karopoulos, C., M.J. Rowley, C.J. Handley, and R.A. Strugnell. 1995. Antibody reactivity to mycobacterial 65 kDa heat shock protein: relevance to autoimmunity. *J. Autoimmun.* 8:235–248.
38. Staton, J.M., D.E. Dench, B. Currie, D.R. Fitzpatrick, R.P. Himbeck, R. Allen, J. Bruce, B.W. Robinson, and H. Bielefeldt-Ohmann. 1995. Expression and immune recognition of stress proteins in sarcoidosis and other chronic interstitial lung diseases. *Immunol. Cell Biol.* 73:23–32.
39. Benoist, C., and D. Mathis. 2001. Autoimmunity provoked by infection: how good is the case for T cell epitope mimicry? *Nat. Immunol.* 2:797–801.
40. Lo, W.-F., A.S. Woods, A. Decloux, R.J. Cotter, E.S. Metcalf, and M.J. Soloski. 2000. Molecular mimicry mediated by MHC class Ib molecules after infection with Gram-negative pathogens. *Nat. Med.* 6:215–218.
41. Amital, H., I. Klemperer, M. Blank, Y. Yassur, A. Palestine, R.B. Nussenblatt, and Y. Shoenfeld. 1992. Analysis of autoantibodies among patients with primary and secondary uveitis: high incidence in patients with sarcoidosis. *Int. Arch. Allergy Immunol.* 99:34–36.
42. Inaba, K., M. Inaba, M. Naito, and R.M. Steinman. 1993. Dendritic cell progenitors phagocytose particulates, including bacillus Calmette-Guerin organisms, and sensitize mice to mycobacterial antigens in vivo. *J. Exp. Med.* 178:479–488.
43. Tailleux, L., O. Schwartz, J.L. Herrmann, E. Pivert, M. Jackson, A. Amara, L. Legres, D. Dreher, L.P. Nicod, J.C. Gluckman, et al. 2003. DC-SIGN is the major *Mycobacterium tuberculosis* receptor on human dendritic cells. *J. Exp. Med.* 197:121–127.
44. Chensue, S.W., K.S. Warmington, J.H. Ruth, P. Lincoln, and S.L. Kunkel. 1995. Cytokine function during mycobacterial and schistosomal antigen-induced pulmonary granuloma formation. Local and regional participation of IFN-gamma, IL-10, and TNF. *J. Immunol.* 154:5969–5976.
45. Wangoo, A., T. Sparer, I.N. Brown, V.A. Snewin, R. Janssen, J. Thole, H.T. Cook, R.J. Shaw, and D.B. Young. 2001. Contribution of Th1 and Th2 cells to protection and pathology in experimental models of granulomatous lung disease. *J. Immunol.* 166:332–339.
46. Baughman, R.P., A.S. Teirstein, M.A. Judson, M.D. Rossman, H. Yeager Jr., E.A. Bresnitz, L. DePalo, G. Hunninghake, M.C. Iannuzzi, C.J. Johns, G. McLennan, D.R. Moller, et al. Case Control Etiologic Study of Sarcoidosis (ACCESS) research group. Clinical characteristics of patients in a case control study of sarcoidosis. 2001. *Am. J. Respir. Crit. Care Med.* 164:1885–1889.
47. American Thoracic Society, Centers for Disease Control and Prevention. 2000. Diagnostic standards and classification of tuberculosis in adults and children. *Am. J. Respir. Crit. Care Med.* 161:1376–1395.
48. Cotter R.J. The new time-of-flight mass spectrometry. 1999. *Analytic Chem. News and Features* 4:445A–451A.
49. Marzilli, L., T.R. Golden, R.J. Cotter, and A.S. Woods. 2000. Peptide sequence information derived by pronase digestion and ammonium sulfate in-source decay matrix-assisted laser desorption/ionization time-of-flight mass spectrometry. *J. Am. Soc. Mass Spectrom.* 11:1000–1008.
50. Pappin, D.J.C., P. Hojrup, and A.J. Bleasby. 1993. Rapid identification of proteins by peptide-mass fingerprinting. *Curr. Biol.* 3:327–341.
51. Johnsson, K., W. Froland, and P. Schultz. 1997. Overexpression, purification, and characterization of the catalase-peroxidase KatG from *Mycobacterium tuberculosis*. *J. Biol. Chem.* 272:2834–2840.
52. Xiang, Q., and R.V. Lloyd. 2003. Recent developments in signal amplification methods for in situ hybridization. *Diagn. Mol. Pathol.* 12:1–13.
53. Kerstens, H.M., P.J. Poddighe, and A.G. Hanselaar. 1995. A novel in situ hybridization signal amplification method based on the deposition of biotinylated tyramine. *J. Histochem. Cytochem.* 43:347–352.
54. Zerbi, P., A. Schonau, S. Bonetto, A. Gori, G. Costanzi, P. Duca, and L. Vago. 2001. Amplified in situ hybridization with peptide nucleic acid probes for differentiation of *Mycobacterium tuberculosis* complex and nontuberculous *Mycobacterium* species on formalin-fixed, paraffin-embedded archival biopsy and autopsy samples. *Am. J. Clin. Pathol.* 116:770–775.